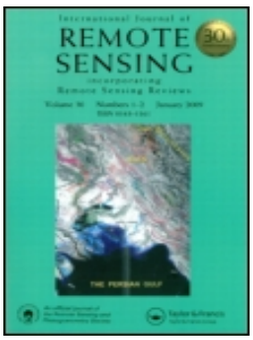

International Journal of Remote Sensing

ISSN: 0143-1161 (Print) 1366-5901 (Online) Journal homepage: https://www.tandfonline.com/loi/tres20

Historical and future land-cover changes in the Upper Ganges basin of India

G.M. Tsarouchi, A. Mijic, S. Moulds & W. Buytaert

To cite this article: G.M. Tsarouchi, A. Mijic, S. Moulds & W. Buytaert (2014) Historical and future land-cover changes in the Upper Ganges basin of India, International Journal of Remote Sensing, 35:9, 3150-3176, DOI: 10.1080/01431161.2014.903352

To link to this article: https://doi.org/10.1080/01431161.2014.903352

Published online: 02 Apr 2014.

International Journal of Remote Sensing, 2014
Vol. 35, No. 9, 3150–3176, http://dx.doi.org/10.1080/01431161.2014.903352

Taylor & Francis
Taylor & Francis Group

Historical and future land-cover changes in the Upper Ganges basin of India

G.M. Tsarouchi[a,b]*, A. Mijic[a], S. Moulds[a,b], and W. Buytaert[a,b]

[a]*Department of Civil and Environmental Engineering, Imperial College London, London, UK;*
[b]*Grantham Institute for Climate Change, Imperial College London, London, UK*

(*Received 5 July 2013; accepted 8 February 2014*)

The green revolution represents one of the greatest environmental changes in India over the last century. The Upper Ganges (UG) basin is experiencing rapid rates of change of land cover and irrigation practices. In this study, we investigated the historical rate of change and created future scenario projections by means of 30 m-resolution multi-temporal Landsat 5 Thematic Mapper and Landsat 7 Enhanced Thematic Mapper Plus data of the UG basin. Post-classification change analysis methods were applied to Landsat images in order to detect and quantify land-cover changes in the UG basin. Subsequently, Markov chain analysis was applied to project future scenarios of land-cover change. Fifteen different scenarios were generated based on historic land-cover change. These scenarios diverged in terms of future projections, highlighting the dynamic nature of the changes. This study has shown that between the years 1984 and 2010 the main land-cover change trends are conversion from shrubs to forest (+4.7%), urbanization (+5.8%), agricultural expansion (+1.3%), and loss of barren land (–9.5%). The land-cover change patterns in the UG basin were mapped and quantified, showing the capability of Landsat data in providing accurate land-cover maps. These results, in combination with those derived from the Markov model, provide the necessary evidence base to support regional land-use planning and develop future-proof water resource management strategies.

1. Introduction

In recent decades, India has undergone substantial environmental change. India's green revolution was initiated by the introduction, in the mid-1960s, of high-yielding varieties of rice and wheat across Latin America and Asia (Singh 2000; Evenson and Gollin 2003), with the aim of increasing food security and promoting sustainable economic development on these continents (Pinstrup-Andersen and Hazell 1985). Combined with the expansion of agricultural land area to meet the demand of a rapidly increasing population, the green revolution has enabled India to become self-sufficient in food grains (Singh 2000; Sen Roy et al. 2007). In the initial stages of the green revolution, the growth in agricultural area was achieved through widespread deforestation (Rai, Sharma, and Sundriyal 1994; Singh 2000). However, since the beginning of the 1990s, India has pursued a policy of afforestation and reforestation combined with conservation of its existing resources (Ravindranath, Chaturvedi, and Murthy 2008).

Land-cover change affects the water resources of northern India in complex ways. Several studies have identified a strong feedback mechanism between soil moisture and precipitation

*Corresponding author. Email: g.tsarouchi11@imperial.ac.uk

(e.g. Meehl 1994; Koster et al. 2004; Seneviratne et al. 2010). This arises because the amount of soil moisture on the land surface affects the partitioning between sensible and latent heat: greater soil moisture increases the latent heat flux, reducing the amount of energy available to warm the air at the near surface (Pitman 2003). Modelling carried out by Meehl (1994) showed that the increase in soil moisture at the land surface due to irrigation influenced the strength of the Asian monsoon. A study by Sen Roy et al. (2011) linked soil moisture from irrigation to increased precipitation during the dry season. The pressure on water resources in India is likely to increase further, with forecast population growth together with continued economic progress. Consequently it is essential to understand historic trends in land-cover change and make valid predictions of future change in order to understand its effects on water resources and improve water security in the region.

One of the most successful applications of remote-sensing techniques is recording land-use/cover changes through time (Christensen et al. 1988). The Landsat programme, one of NASA's major Earth observation initiatives, has been providing a nearly continuous record of the global land surface change since its inception in 1972 (Cohen and Goward 2004). Landsat 5 was launched in 1984 and ended image acquisition in 2013. Landsat 7 was launched in 1999 and continues in operation today. The fixed acquisition schedule these follow (the satellite revisits the same spot on Earth every 16 days) has provided a long-term record, representing the longest and one of the most consistently available datasets in remote-sensing history. Its use has extended knowledge of land-surface processes across spatial and temporal scales and enhanced scientific research (Cohen and Goward 2004). Satellite images are widely used today in land-cover classification and change detection analysis (Ehlers et al. 1990; Westmoreland and Stow 1992; Harris and Ventura 1995; Yeh and Li 1999). However, as a result of management decisions and operational errors, the availability of Landsat images for northern India is poor (Goward, Arvidson, and Williams (2006). Furthermore, heavy cloud cover during the monsoon (June–September) means that satellite images for this season frequently cannot be used (Thenkabail, Schull, and Turral 2005; Goward, Arvidson, and Williams (2006). Because of these shortcomings, the dynamics of land-cover changes over the Indian subcontinent remain poorly studied.

Recently published regional land-use mapping studies tend to focus on the cities of central and southern India. Jat, Garg, and Khare (2008) used statistical classification approaches in high-resolution (5–25 m) satellite images acquired over the period 1977–2005 to study the urban expansion of Ajmer City in India. To establish a relationship between urbanization and its causative factors, they applied multivariate statistical techniques and found that, by 2051, the built-up area in the region would increase by almost 100% when projected using present trends. Bhatta (2009) classified satellite images acquired by Landsat and the Indian Remote Sensing (IRS) sensor into urban and non-urban to examine the urbanization pattern of Kolkata, India. The results showed that although the population growth rate has been declining, there is a clear indication of dispersed development of the city. Rajitha et al. (2010) mapped the land-cover changes occurring in their study area in Andhra Pradesh, India, during the period 1990–2005. They quantified the changes based on normalized difference vegetation index (NDVI) image differencing and post-classification change analysis, and developed future scenarios for 2010 based on Markov chains. Moghadam and Helbich (2013) developed land-cover maps for the years between 1973 and 2010 based on Landsat imagery for the city of Mumbai in India. Furthermore, they applied an integrated Markov Chains Cellular Automata (MC–CA) urban growth model to project urban expansion for the years 2020–2030.

Along with the studies mentioned above, several other recent studies (Sheeja et al. 2011; Bhagyanagar et al. 2012; Rahman et al. 2012; Raja et al. 2013) focusing on India

have mainly investigated changes in small-scale systems, mostly related to urbanization. Therefore, investigating the dynamics of land-cover changes in a large-scale system, such as the Upper Ganges (UG) basin, is a challenge for this study.

In recent years several dynamic-process-based land-cover-change models have been developed, such as cellular automata and econometric and agent-based models (see review articles of Parker et al. (2003), Verburg et al. (2009), and Sohl and Claggett (2013)). These models can represent human decision-making and environmental management policies while taking into account the processes that drive land-cover change. Over recent years, a new approach based on combining elements of different modelling techniques has become popular. An increased number of land-use/land-cover (LULC) change modelling tools have been linked with each other, leading to multidisciplinary modelling frameworks. For instance, Claessens et al. (2009) coupled the land-use change model conversion of land use and its effects (CLUE) (Verburg et al. 2002) with the landscape process model LAPSUS (Landscape Process Modelling at Multi-Dimensions and Scales; Schoorl, Veldkamp, and Bouma 2002), which simulates water and tillage erosion and sedimentation, to model interactions and feedbacks between land-use change and geomorphic processes. Renwick et al. (2013) combined the Common Agricultural Policy Regionalized Impact (CAPRI) modelling system and Dyna-CLUE models to examine the potential impact of agricultural land-use conversion and trade policy reform on land use across the European Union (EU). Verburg, Eickhout, and Meijl (2008) presented a scenario-based modelling approach to support policy discussions as developed in the Eururalis project (Westhoek, van den Berg, and Bakkes 2006), and to link global level developments influencing land use to local level impacts; three models are linked together: an extended version of the global economic model GTAP (Global Trade Analysis Project), the IMAGE (Integrated Model to Assess the Global Environment) model, and CLUE-s.

All these different approaches have substantially improved the representation of complex systems by offering different levels of modelling complexity dependent on input data availability (Sohl and Claggett 2013). However, the data requirements of dynamic-based models do not allow for their implementation in a data-scarce region such us our study area. Furthermore, a recent study by Tayyebi, Tayyebi, and Khanna (2014) compared two different types of land-use-change models (artificial neural networks and spatial logistic regression models) to categorize and measure various dimensions of uncertainties. They found that the uncertainty in land-use-change modelling originating from data uncertainties is greater than that originating from model parameter uncertainties. Thus, to overcome the data limitation which would increase our modelling uncertainty, an empirically fitted model (Markov chains) was selected.

This paper aims to capture historical and future spatio-temporal trends in land-cover change by modelling the dynamics of land-cover change and developing future projection scenarios. The methodology combines the analysis of 30 m-resolution multi-temporal Landsat 5 Thematic Mapper (TM) and Landsat 7 Enhanced Thematic Mapper plus (ETM+) data with Markov modelling to detect, quantify, and analyse land-cover changes between 1984 and 2010, and to create future projections of change in the UG basin of India. Hypothetical future projection scenarios of land cover are developed using Markov chain analysis and by generating transition probability matrices, which indicate transition potentials from one land-cover class to another. The results are expected to enhance progress in identifying and understanding the temporal dynamics of climate–surface–groundwater fluxes as a function of land-cover changes.

2. Data

2.1. Study area

The study region is the UG basin located in Northern India (Figure 1), which covers an area of 87,000 km^2. The elevation ranges from 7400 m in the Himalayan mountain peaks to 90 m in the plains. When the River Ganges reaches the plains, it becomes subject to a vast irrigation demand as 410 million people are dependent on it to cover their daily needs (Verghese 1993). Around 60% of the basin is occupied by agriculture (main crop types include wheat, maize, rice, sugarcane, bajra, and potato), while 20% is covered by forests, mostly in the upper mountains, and approximately 2% in the mountain peaks is permanently covered with snow (Bharati and Jayakody 2010). The annual average rainfall in the UG basin ranges between 550 and 2500 mm (Bharati and Jayakody 2010), and a major part of the rains is due to the southwesterly monsoon that prevails from July to late September (Figure 2). The Ganges basin is the most densely populated river basin in the world, with an average population density of 520 km^{-2}. Between 1991 and 2001, the urban population of India increased by 32% and this trend is likely to continue, making the study area subject to rapid land-cover changes (O'Keeffe et al. 2012). According to the 2011 census (Office of the Registrar General, Census Commissioner and India 2011), the population of India increased by more than 181 million from 2001 to 2011, reaching 1.21 billion.

2.2. Remote-sensing data

Landsat 5 TM and Landsat 7 ETM+ images, 77 in total, for the month of October in 1984, 1990, 1998, 2000, 2002, 2004, 2006, 2008, and 2010, were acquired from the US Geological Survey Global Visualization Viewer. Prior to the analysis, the images were

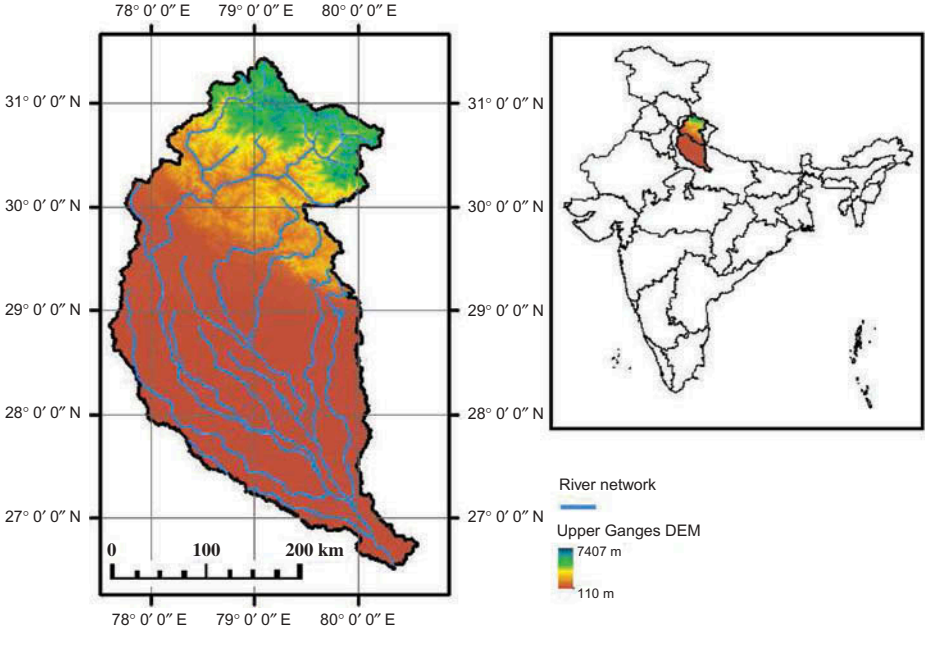

Figure 1. Location map of the study area in northern India and digital elevation model (DEM) of the UG basin showing the range of elevations (m altitude).

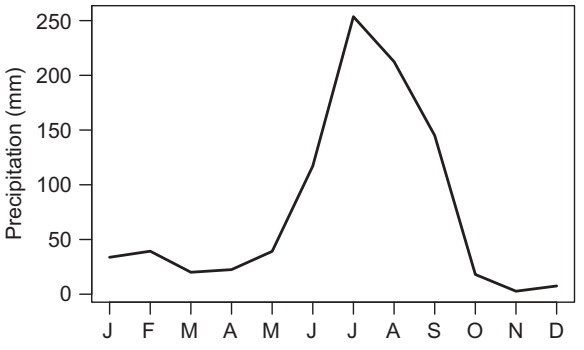

Figure 2. Precipitation monthly climatology in the UG basin based on Tropical Rainfall Measuring Mission (TRMM) satellite data product 3B42v7A. The main amount of rainfall received over the study area is due to the southwesterly monsoon, which occurs from July to late September.

co-registered to UTM projection zone 44N, WGS 1984 datum, and corrected for radiometric and atmospheric effects. Then the images were classified using a maximum likelihood classifier method with pixel training data sets, resulting in land-cover maps of eight different classes.

2.3. Field data

The total of 400 validation points for each land-cover map were selected by visual interpretation of high-resolution imagery on Google Earth, along with ground truth data collected after a survey of the site in 2012. In addition, online data from the Global Geo-Referenced Field Photo Library (University of Oklahoma 2011) were used to relate land cover to the supervised classifications results. The field data were also used in the land-cover change detection analysis to distinguish between areas with and areas without change. All images from Google Earth and from the Global Geo-Referenced Field Photo Library are labelled with the acquisition date, and for the validation we selected images acquired in the same month as the Landsat images. When that was not possible, the images selected were acquired within one month's difference of the satellite image acquisition date.

3. Methodology

The data analysis is divided into three phases: (1) image processing and land-cover-map preparation; (2) land-cover-change detection and analysis; and (3) stochastic modelling and future projections of land-cover change.

3.1. Image processing and classification

Land-cover maps were produced by applying supervised classification techniques to the Landsat images with a 30 m ground resolution. The accuracy of the classification is highly dependent on the quality of the satellite data interpreted. Especially in cases where multi-temporal images (i.e. not acquired on the same date) are to be analysed and compared, a primary pre-processing task is necessary, in which radiometric and atmospheric corrections are applied to each image.

To overcome the lack of detailed *in situ* field data of atmospheric optical properties at the time of image acquisition, an image-based dark object subtraction (DOS) method was used (Chavez 1989, 1996; Moran et al. 1992). This method is the simplest yet most widely used approach, suitable for areas with dense vegetation (Spanner et al. 1990; Ekstrand 1994; Jakubauskas 1996; Huguenin et al. 1997).

After these corrections, supervised classifications were implemented using the maximum likelihood algorithm. All six optical bands of the TM5/ETM+ sensors were used (bands 1–5, 7). The steps followed for the supervised classifications included: (1) the selection of training regions; (2) the calculation of regional statistics in order to avoid overlapping between different classes; (3) the evaluation of each class; and (4) the application of the maximum likelihood classifier. A total of 160 training regions, evenly distributed among the land-cover classes, were chosen by means of on-screen selection for each image to ensure adequate representation of all spectral classes in the training statistics (Wu et al. 2006). Land-cover classes were defined as water, forest, shrubs, grass, crops, urban, snow, and barren.

The NDVI, proposed by Rouse et al. (1974), was used as an additional data layer in the classification procedure to enhance detection among various land-cover classes and also to reduce the shadow effect due to the mountainside slopes. NDVI is the most commonly used and well-known vegetation index and, as previously mentioned by Song et al. (2001), has been used in several studies to monitor vegetation dynamics (Sader 1987; Lenney et al. 1996; Michener and Houhoulis 1997).

The classification algorithm may sometimes misclassify pixels, either due to an analyst's error during the training model procedure or to a spectral overlap between different land-cover types. Hence, one of the most important steps to be followed after the classification of remotely sensed data is accuracy assessment of the classification, which determines the quality of the information derived from satellite images. The error matrix is the most common method for accuracy assessment, as it is the only way to effectively compare two maps quantitatively (Lu et al. 2004; Congalton and Plourde 2002). The matrix consists of a square array of numbers, or cells, which represent the number of sample units assigned to each land-cover type as compared to what is on the ground (Congalton and Plourde 2002). Ground truth data collection is the first and most important step in accuracy assessment, since the whole procedure will be pointless if the reference data are not trustworthy (Congalton 2010). After developing the error matrix, the overall accuracy and kappa coefficient were calculated for each classification using techniques described in Congalton (1991).

The total of 200 samples for each image date were obtained through visual interpretation of the area. This was aided by previous experience in identifying features on the image based on what we knew existed on the ground, determined by direct field observation and interpretation using Google Maps. These 200 samples were split by random sampling into training and validation datasets, ensuring that all land-cover types were equally represented in each dataset. The training dataset (160 points, evenly distributed between the land-cover classes) was used to calibrate the model, while the validation dataset (40 points, evenly distributed between the land-cover classes) was used to test the model's performance. This cross-validation procedure (i.e. repeated random sub-sampling) was carried out 10 times for each image. The final error was estimated as the average of individual errors. Once the cross-validation testing was complete, the 400 validation points (see Section 2.3) were used to test the performance of the model that gave the best accuracy during cross-validation.

3.2. Land-cover-change detection and analysis

In order to detect and quantify the changes in land-cover patterns from 1984 to 2010, a post-classification change analysis approach was followed, based on a cross-tabulation detection method that produces a change matrix where different combinations of change are identified. This allowed us to quantify the changes by knowing how much of a given land-cover type had changed and into what categories, as well as to identify trends in land-cover changes that had taken place in the UG basin since 1984. The classified images were compared on a pixel-by-pixel basis and the accuracy of the change map was the product of the accuracies of the individual classification maps. Hence, this method required a very good level of accuracy in both images (Singh 1989; Lambin and Strahler 1994). In addition, for analysis of the location, type, and rate of change, a set of images indicating the gains and losses per land-cover class was produced.

3.3. Stochastic modelling and future projections

To generate future land-cover scenarios, one of the analytical methods of the stochastic process, Markov chain analysis, was applied. Many studies of land-cover-change analysis use Markov modelling (Drewett 1969; Lever 1973; Bell 1974; Muller and Middleton 1994; Weng 2002; Petit, Scudde, and Lambin 2001; Wu et al. 2006; Liu et al. 2008; Rajitha et al. 2010). These studies were mainly focused on small areas and based on data sampled from fieldwork, existing maps, or aerial photography. The application of Markovian analysis to large-scale systems such as the UG basin is a challenge for this study. The usage of satellite images is expected to reduce uncertainty and improve the analysis. The method is based on the assumption that the driving forces that produced changes in the past will continue to do so in the future. However, this assumption is not always true, especially over long periods, and therefore we chose to apply the method only for the period from 2000 to 2010, where the frequency of available land-cover maps is high (one map every two years). In theory, a given cell of land may change from any type of land cover to any other.

Before applying the Markovian analysis, the method was tested to evaluate its validity for projecting land-cover changes in the UG basin. The three assumptions tested were: (a) land cover is statistically dependent only on land cover during the preceding time period; (b) this dependence is a first-order Markovian dependence; and (c) the system is stationary, meaning that the driving factors causing changes in the past will continue to do so in the future.

More analytically, the first test was a statistical independence test. Land-cover change in an area is characterized by a Markovian process when the land-cover class of any randomly chosen cell is statistically dependent only on the preceding land-cover class and not on any earlier one (Bell 1974). The null hypothesis that land cover at one point in time (t_1) is statistically independent of land cover at the preceding time period (t_0) is being tested. If M is the number of land-cover classes (here $M = 8$), Karl Pearson's χ^2 is calculated with $(M-1)^2$ degrees of freedom:

$$\chi^2 = \sum_i \sum_k \frac{(n_{ik} - \hat{m}_{ik})^2}{\hat{m}_{ik}}, \tag{1}$$

where n_{ik} is the number of cells that transitioned from class i to k over the period 2000–2010, for instance; and m_{ik} is the expected number of cells that transitioned from class i to k under the Markov hypothesis over the same period.

We will call this test K^2 rather than χ^2, to differentiate from its distribution (χ^2). For $(M-1)^2 = 49$ and a critical region of 0.05, values of K^2 less than 66.3 would indicate that the hypothesis of land-cover independence is true.

To calculate $\hat{m}_{ik}$, we applied the Chapman–Kolmogorov equation (Equation (2)). Markovian theory assumes that the probability of transitioning from state 1 to state 3 can be calculated from the probabilities of transitioning from 1 to an intermediate state 2 and then from state 2 to state 3. For instance, the transition probability matrix of the period 2000–2010 can be calculated by multiplying the elements of the 2000–2004 and 2004–2010 matrices:

$$\hat{m}_{ik} = \sum_j \frac{m_{ij} \times m_{jk}}{m_j}, \tag{2}$$

where m_{ij} is the number of cells that transitioned from class i to j in the period 2000–2004; m_{jk} is the number of cells that transitioned from class j to k in the period 2004–2010; and m_j is the number of cells in class j in 2004. The test was applied to all possible transition combinations of the years 2000, 2002, 2004, 2006, 2008, and 2010.

If the data are proved to be statistically dependent, the second test will show whether the dependence is characterized by a first-order Markov dependence or by a higher-order dependence (Weng 2002). The test for the first-order Markovian dependence is a χ^2 goodness of fit test, which compares the observed transition probabilities to the expected transition probabilities in order to judge whether those observed are described by a particular distribution (Weng 2002). Here, the expected transition probabilities are described by a Markovian distribution. The statistic χ^2 is calculated by Equation (4) and is described by a chi-squared distribution. The hypothesis that the data are described by first-order Markovian dependence is true if

$$\chi_c^2 < \chi_{1-n,(M-1)^2}^2, \tag{3}$$

where

$$\chi_c^2 = \sum_i \sum_k \frac{(O_{ik} - E_{ik})^2}{E_{ik}}, \tag{4}$$

where O_{ik} is the transition probability from class i to k in the period 2000–2010, for instance; and E_{ik} is the expected transition probability from class i to k under the Markov hypothesis in the same period.

The third test is a stationarity test. Markov transition probability-based models assume that the probability matrix is stationary over time and space. According to this assumption, changes in land cover for all tested periods between 2000 and 2010 occur as a result of the same transition mechanism. To test this assumption, we will calculate the steady-state probabilities, which show the equilibrium distributions for these periods. These distributions are calculated by multiplying the transition matrices by themselves (Bell 1974; Bourne 1976) until they converge to a matrix with identical rows. The values of the equilibrium matrix represent the amount of each land-cover class at a hypothetical future equilibrium. Furthermore, this shows that the Markovian process is not a simple linear

extrapolation, because the transition potentials change over time as the various transitions reach an equilibrium state.

The matrices of change produced by the post-classification change analysis show the number of cells that have changed from each land-cover class to another. These numbers are converted to probabilities by dividing each element by its equivalent row total. In this study, the probability for each land cover class to change to every other class is represented in a matrix which (with eight land-cover classes, and therefore 64 possible different land cover transitions) is a 64-cell transition matrix for each discrete time period. The rows represent the older land-cover categories and the columns the newer ones. The model applied in this study is a first-order Markov chain, meaning that the probability that a system will be in a given state at a given time (t_1) is dependent only on the current land-cover type of a cell (at time t_0) and not on the land-cover types that previously occupied the cell. The transition predictions can be determined as functions of current land covers. The mathematical structure of this approach is based on probabilities of transition between each pair of land covers i and j. The model has the form

$$n_{t_1} = P \times n_{t_0}, \tag{5}$$

where n_{t_0} and n_{t_0} are vectors representing fractions of each land-cover class at times t_0 and t_1, respectively, and P is a transition probabilities matrix that indicates the probability of moving from one class i at time t_0 to another class j at time t_1. For m land cover classes, P has a dimension of $m \times m$. Each row of the matrix must total 1. Once the initial transition probability matrix is calculated, it can be used to project land-cover changes at any time in the future.

If the date being projected forward is an even multiple of the training period, then the new transition probability matrix is calculated through a simple powering of the base matrix. If the date being projected in the future is not an even multiple of the training period, the derivation of a yearly transition probability matrix is required. Previous studies used a linear algebraic formula of the power root of matrices to generate this annual matrix, but several difficulties arise by this approach as discussed in the study of Takada, Miyamoto, and Hasegawa (2010).

Therefore, in the present study we chose to develop our future scenarios based on even multiples of the training periods.

In this study, all 15 available transition matrices of periods between the years 2000 and 2010 were used to develop different scenarios of the future land-cover status for the year 2020. As the trends in different matrices vary, the future predictions generated are expected not to be the same. It is, by definition, impossible to test the accuracy of a scenario that projects the future; however, to visualize the uncertainty and identify outliers between those 15 future scenarios, we created box-plots which help identify the spread and skewness of future predictions.

4. Results and discussion

4.1. Image processing and classification

Land-cover maps were produced after supervised classification techniques were applied to Landsat images for the years 1984, 1990, 1998, 2000, 2002, 2004, 2006, 2008, and 2010 (Figure 3). The error matrix produced by comparing classification results with ground

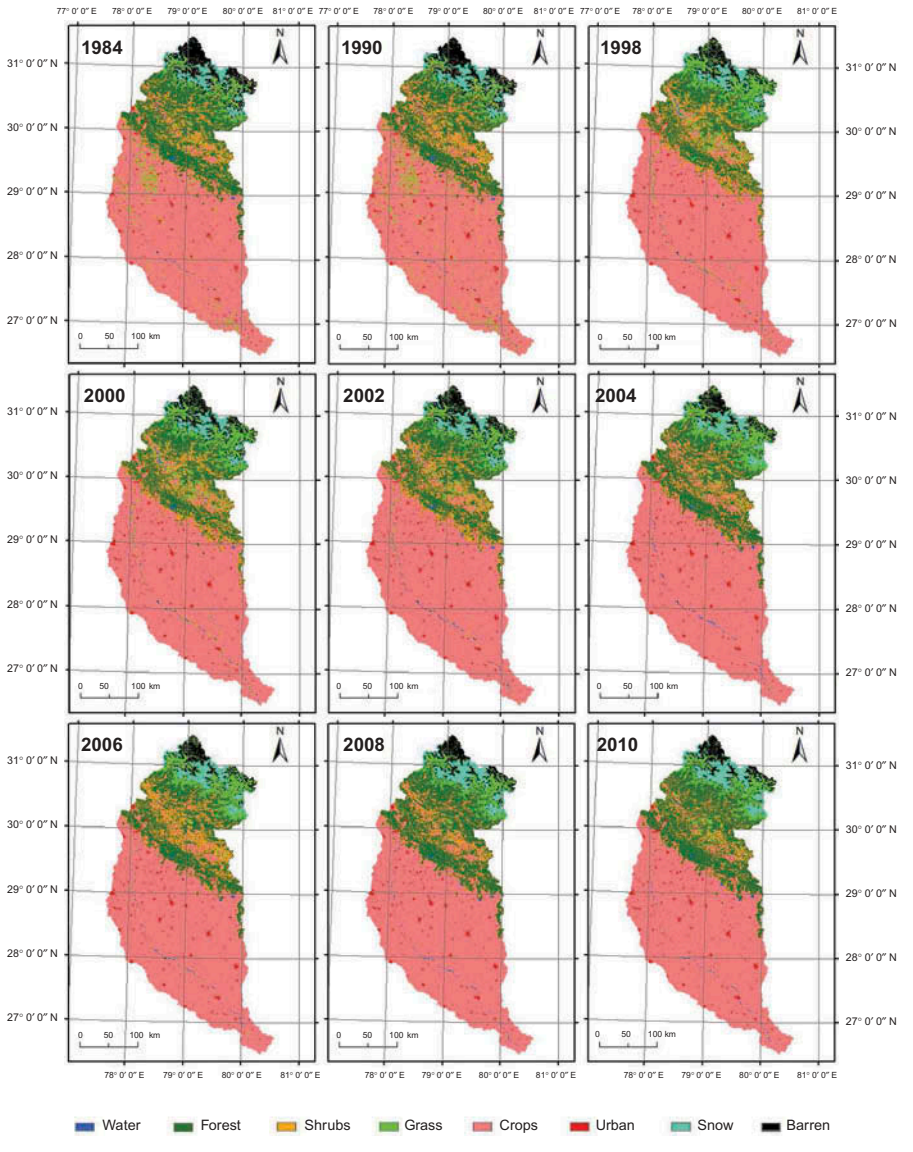

Figure 3. Image classification results for the study years. The eight classes identified are water, forest, shrubs, grass, crops, urban, snow, and barren.

truth data and high-resolution images (Table 1) indicated a sufficient level of accuracy, allowing us to further analyse and study trends in land-cover changes in the UG basin. The highest overall accuracy achieved was 93.73% for the year 2002. The kappa coefficient for that year was 0.91, representing a 91% better agreement than if the classification had been the result of a random assignment. Kappa values greater than 0.80 represent strong agreement (Congalton 1991) and a widely used, minimum level of acceptable accuracy for land-cover classification is 85% (Anderson, Hardy, and Roach 1976).

Table 1. Classification accuracy assessment for each classification based on ground truth data and high-resolution images. The results were produced by applying the techniques described in Congalton (1991).

Image	Overall	Kappa
1984	87.03	0.86
1990	86.88	0.84
1998	87.15	0.86
2000	90.57	0.88
2002	93.73	0.91
2004	93.21	0.90
2006	92.90	0.90
2008	88.86	0.87
2010	91.72	0.91

As no ground truth data or aerial photographs were available for the 1984 and 1990 classifications, validation relied upon expert manual judgement of the classification in the validation points.

4.2. *Land-cover-change detection and analysis*

According to the 1984 classification (Figure 3), areas in the north of the UG basin (Himalayas) were either barren or covered by snow. The central and northern parts of the catchment were dominated by forests. In the central areas, a combination of dense vegetation and crops was identified along with barren and grassland. Most of the urban and agricultural areas in the basin are located towards the south, in the plains of the UG basin.

Looking at the changes in land-cover proportions over the periods examined (Figures 4 and 5), crops increased from 1984 to 2006 but from 2006 to 2010 they decreased; however, the overall change from 1984 to 2010 was an increase of 1.3%. The trends observed in the forest proportion follow the opposite direction: forest decreased from 1984 to 1998 but from 1998 to 2010 it increased, achieving a total increase of 4.7% from 1984 to 2010. Shrub coverage increased from 1984 to 2000 but from 2000 onwards it decreased and showed an overall change of –11.6% from 1984 to 2010. Grass and barren lands did not show a stable trend of increase or decrease in the periods examined between 1984 and 2010; nevertheless, they reduced from 1984 to 2010 by 9.0% and 9.5%, respectively. Urban coverage was expanded from 1984 onwards, and the total increase during the 1984–2010 period was 5.8%.

Figure 7 shows the contributors to net change from a perspective of land cover. The main contributor to the net change in forest area was conversion to/from shrubs. Barren land changed due to conversion to/from water, grass, and snow. Crop change occurred due to conversion to/from water, shrubs, grass, and barren. Grass change was due to conversion to/from water, snow, and barren land. The main contributors to changes in shrubs were forest, snow, and barren land. Finally, shrubs, grass, and barren land were the main contributors to snow coverage change.

Landsat classification indicated that the share of forested areas decreased by 4.1% from 1984 to 1990 (Figure 4), the same trend observed by Gulati and Sharma (2000). This loss can be explained by the conversion to agricultural and other uses, such as heavy grazing and forest fires driven by population growth. During the period 1984–1990,

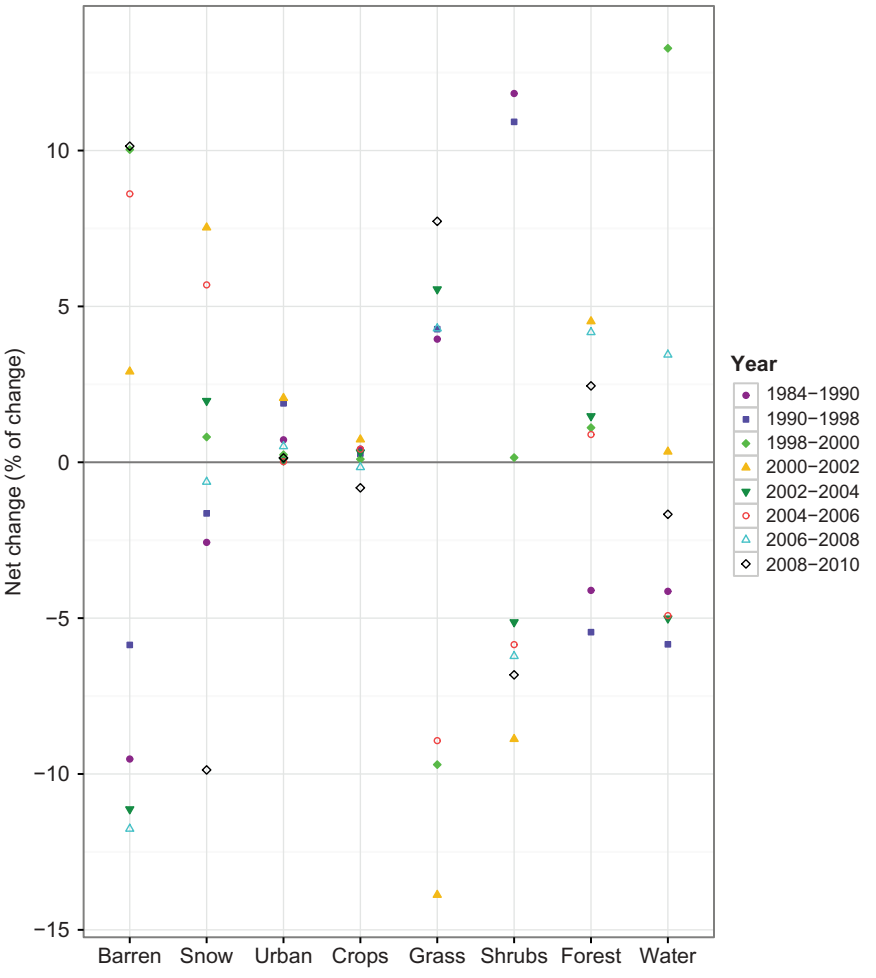

Figure 4. Changes in land-cover proportions over the periods examined, based on the image classification results.

agriculture in the UG basin increased by 0.4%, urban by 0.7%, grass by 4%, and shrubs by 11.8%. According to Figure 7, the main reason for loss of forest during the 1984–1990 period was conversion to shrubs.

The trend in forested area between 2000 and 2006 shows an increase of 7% (Table 2). This is consistent with reports that investigated forest growth in India over that period, specifically in the states of Uttar Pradesh and Uttarakhand, the areas of our study. Specifically, the State of Forest Report by the Forest Survey of India (2009) (reports of the years 2001 and 2009) showed, for the states of Uttar Pradesh and Uttarakhand, an increase of 4.33% and 3.17%, respectively, between 2001 and 2007. In addition, the Global Forest Resources Assessment by FAO (2010) showed an increase of 0.70% in the forest cover area of India from 2000 to 2005, and an increase of 0.21% from 2005 to 2010 (Figure 5).

In order to analyse the location, type, and rate of changes, a set of images indicating the gains and losses per land-cover class was produced. Figure 6 shows indicative changes

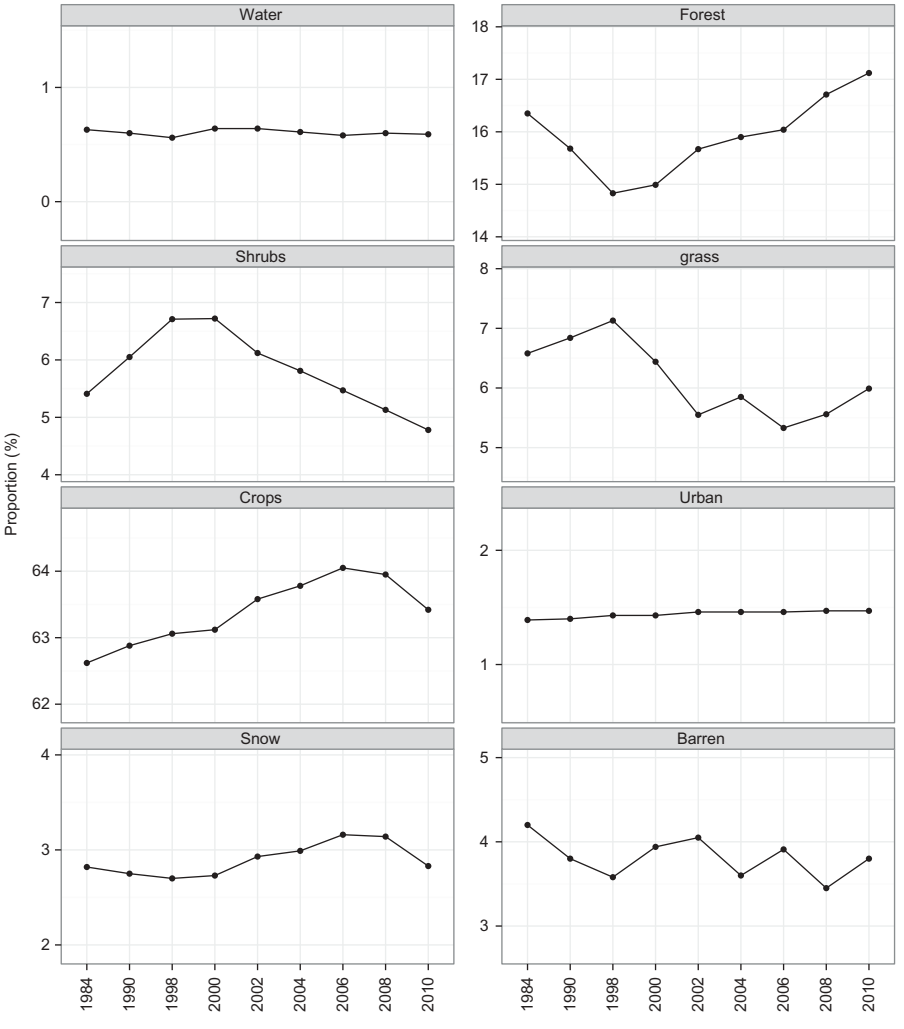

Figure 5. Land-cover proportions based on the image classification results.

Table 2. Land-cover proportions for the developed land-cover maps.

Image	Water	Forest	Shrubs	Grass	Crops	Urban	Snow	Barren
1984	0.63	16.35	5.41	6.58	62.62	1.39	2.82	4.20
1990	0.60	15.68	6.05	6.84	62.88	1.40	2.75	3.80
1998	0.56	14.83	6.712	7.13	63.06	1.43	2.70	3.58
2000	0.64	14.99	6.72	6.44	63.12	1.43	2.73	3.94
2002	0.64	15.67	6.12	5.55	63.58	1.46	2.93	4.05
2004	0.61	15.90	5.81	5.85	64.78	1.46	2.99	3.60
2006	0.58	16.04	5.47	5.33	64.05	1.46	3.16	3.91
2008	0.60	16.71	5.13	5.56	63.95	1.47	3.14	3.45
2010	0.59	17.12	4.78	5.99	63.42	1.47	2.83	3.80

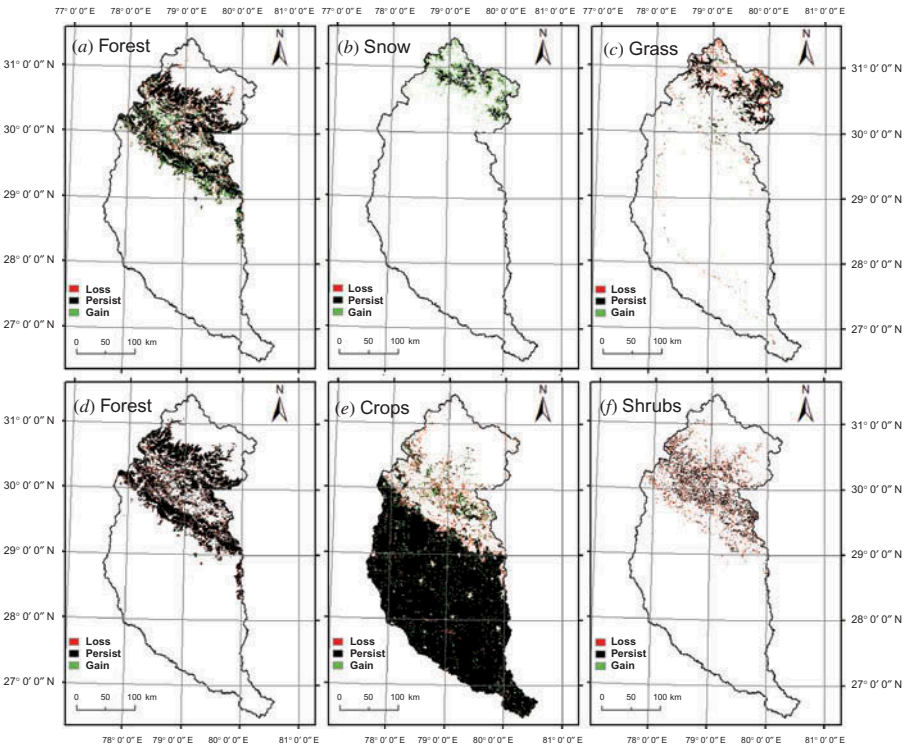

Figure 6. Indicative gains, losses, and areas of land-cover persistence for: (*a*) forest during the period 1998–2010; (*b*) snow during the period 2000–2006; (*c*) grass during the period 2000–2006; (*d*) forest during the period 1984–1998; (*e*) crops during the period 1984–1990; and (*f*) shrubs during the period 1998–2010.

for the land-cover types forest, snow, grass, crops, and shrubs. During the period 1984–1998, the forest proportion decreased in the basin mainly in its northern parts (Figure 6(*d*)). In contrast, during the period 1998–2010, this proportion increased (Figure 6(*a*)). The crop proportion increased during the period 1984–1990 in the middle and southern parts of the basin, but also increased towards the northern areas near the Himalayan foothills. During the period 2000–2006, grass coverage was reduced in the northern part of the study area, while during the same period, snow cover was increased (Figures 6(*b*) and 6(*c*)). According to Figure 7, the most important contributor to the increase in snow observed during that period was conversion from grassland.

Trends from the literature in other locations in India, such as Kerala and Haryana, for the period 1965–1996 confirm the intensification and expansion of cultivated land and the decrease in barren land (Indian National Science Academy, Chinese Academy of Sciences, and US National Academy of Sciences 2001). According to Rao and Pant (2001), who studied a small watershed in the mid-elevation zone of the central Himalayas, (India) between 1986 and 1996, the annual deforestation rate was 0.57%. During this period, intensification of cultivated land and conversion of natural forests and grazing lands to agriculture, as well as a constant thinning of available forest, was recorded. Semwal et al. (2004) reported an increase in agricultural land use by 30% during the period 1963–1993, at the cost of a loss of 5% of forest area in the Pranmati watershed (Uttar Pradesh, India).

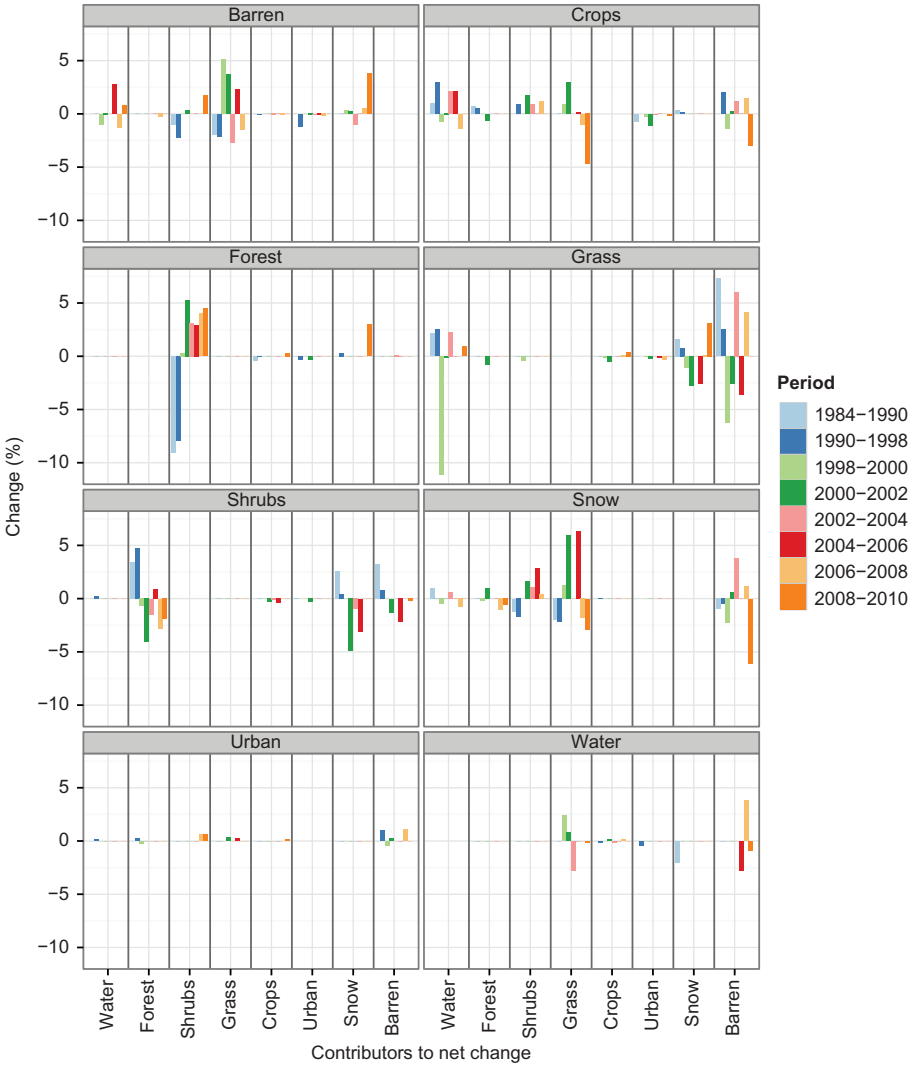

Figure 7. Bar plots illustrating the contributors to net change from a perspective of land cover. A positive value corresponds to land-cover types that contributed to increase in the proportion of a particular class during the study periods. A negative value corresponds to land-cover types to which the particular class was converted.

4.3. Stochastic modelling and future projections

Indicative transition probabilities for the periods 2000–2004, 2000–2010, and 2004–2010 are presented in Tables 3–5. Under the Markovian hypothesis, the expected transition probability matrices for different periods between 2000 and 2010 were calculated (Table 6) by applying the Chapman–Kolmogorov equation (Equation (2)). All Carl Pearson K^2 values derived are shown in Table 8. Since all values were greater than the critical figure 66.3, the null hypothesis that land cover at one point in time (t_1) is statistically independent of land cover at the preceding time period (t_0) was rejected.

Table 3. Transition probabilities, 2000–2004.

	Water	Forest	Shrubs	Grass	Crops	Urban	Snow	Barren
Water	0.2351	0.1813	0.0729	0.1228	0.3367	0.0005	0.0121	0.0386
Forest	0.0017	0.8528	0.0910	0.0173	0.0366	0.0001	0.0001	0.0004
Shrubs	0.0045	0.6175	0.2482	0.0173	0.1115	0.0001	0.0004	0.0005
Grass	0.0220	0.0345	0.0132	0.7275	0.1213	0.0001	0.0082	0.0732
Crops	0.0019	0.0155	0.0092	0.0033	0.9679	0.0020	0.0001	0.0001
Urban	0.0010	0.0016	0.0006	0.0006	0.0945	0.9015	0.0001	0.0001
Snow	0.0009	0.0001	0.0001	0.0575	0.0001	0.0001	0.8959	0.0453
Barren	0.0051	0.0001	0.0001	0.2385	0.0019	0.0001	0.1539	0.6003

Table 4. Transition probabilities, 2000–2010.

	Water	Forest	Shrubs	Grass	Crops	Urban	Snow	Barren
Water	0.2069	0.2577	0.0633	0.0586	0.3631	0.0004	0.0209	0.0291
Forest	0.0009	0.8955	0.0733	0.0073	0.0225	0.0001	0.0001	0.0003
Shrubs	0.0053	0.6701	0.2218	0.0089	0.0931	0.0001	0.0002	0.0005
Grass	0.0147	0.0451	0.0286	0.7108	0.0849	0.0001	0.0175	0.0983
Crops	0.0017	0.0155	0.0134	0.0037	0.9654	0.0001	0.0001	0.0001
Urban	0.0001	0.0001	0.0003	0.0001	0.0001	0.9990	0.0002	0.0001
Snow	0.0005	0.0001	0.0001	0.0040	0.0001	0.0001	0.9706	0.0245
Barren	0.0026	0.0011	0.0003	0.0583	0.0028	0.0001	0.3344	0.6004

Table 5. Transition probabilities, 2004–2010.

	Water	Forest	Shrubs	Grass	Crops	Urban	Snow	Barren
Water	0.3137	0.0891	0.0096	0.1193	0.4375	0.0032	0.0212	0.0064
Forest	0.0017	0.8804	0.0824	0.0047	0.0304	0.0002	0.0001	0.0001
Shrubs	0.0050	0.5860	0.3015	0.0152	0.0916	0.0003	0.0003	0.0001
Grass	0.0092	0.0671	0.0211	0.6163	0.0323	0.0002	0.0892	0.1646
Crops	0.0020	0.0111	0.0114	0.0065	0.9665	0.0023	0.0001	0.0001
Urban	0.0001	0.0010	0.0008	0.0002	0.0840	0.9137	0.0001	0.0001
Snow	0.0009	0.0001	0.0003	0.0133	0.0001	0.0001	0.9533	0.0319
Barren	0.0021	0.0029	0.0008	0.1102	0.0018	0.0002	0.1803	0.7017

Table 6. Expected values of transition probabilities for 2000–2010 under Markov hypothesis.

	Water	Forest	Shrubs	Grass	Crops	Urban	Snow	Barren
Water	0.1597	0.1856	0.1031	0.1038	0.3143	0.0337	0.0413	0.0585
Forest	0.0458	0.6823	0.1985	0.0226	0.0377	0.0051	0.0034	0.0047
Shrubs	0.0615	0.5662	0.2147	0.0285	0.1077	0.0122	0.0040	0.0052
Grass	0.0835	0.0476	0.0356	0.3883	0.1005	0.0109	0.1268	0.2068
Crops	0.1361	0.0392	0.0849	0.0472	0.6230	0.0660	0.0019	0.0018
Urban	0.0210	0.0060	0.0129	0.0074	0.0957	0.8561	0.0005	0.0005
Snow	0.0099	0.0016	0.0014	0.0445	0.0003	0.0004	0.8713	0.0707
Barren	0.0299	0.0062	0.0054	0.1810	0.0025	0.0008	0.3054	0.4687

The χ^2 goodness of fit test for the first-order Markovian dependence gave values of χ^2, as shown in Table 8. For 49 degrees of freedom and a 5% level of significance, the critical value of χ^2 was equal to 33.93. The dependence was therefore characterized by a first-order Markovian dependence, in all cases.

Table 7 and Figure 8 show the equilibrium distributions of land cover for all periods tested, used for analysis of the stationarity of the system. These distributions were calculated by matrix powering (Bourne 1976). According to that method and starting from an initial land-cover distribution n, the iteration $n,\ n \times P,\ n \times P^2,\ n \times P^3,\ldots$, converges to a unique stationary distribution. The transition matrices (P) are multiplied by themselves (Bell 1974; Bourne 1976) until they converge to a matrix with identical rows. The obtained values indicate the amount of each land-cover class at a hypothetical future equilibrium. Some of the distributions are quite similar to each other but the results do not provide evidence that the system is stationary, since not all of them are similar. As other studies have shown, transitions are often not constant over long periods.

Table 7. Steady-state probabilities calculated by multiplying the transition matrices by themselves (matrix powering, Bourne (1976)) until they converge to a matrix with identical rows. The values represent the proportion of each land-cover class at a hypothetical future equilibrium.

	Water	Forest	Shrubs	Grass	Crops	Urban	Snow	Barren
2000–2002	0.0045	0.2490	0.0466	0.0309	0.5595	0.0210	0.0573	0.0312
2002–2004	0.0032	0.1724	0.0319	0.0341	0.6442	0.0909	0.0139	0.0095
2004–2006	0.0020	0.1515	0.0863	0.0232	0.5776	0.1218	0.0256	0.0120
2006–2008	0.0025	0.1792	0.0160	0.0254	0.3051	0.0952	0.3181	0.0585
2008–2010	0.0044	0.2622	0.0458	0.0740	0.4187	0.0109	0.1264	0.0575
2002–2006	0.0022	0.1736	0.0632	0.0283	0.6123	0.0953	0.0183	0.0068
2002–2010	0.0026	0.2618	0.0363	0.0336	0.4413	0.0130	0.1910	0.0204
2004–2010	0.0029	0.2334	0.0354	0.0324	0.4113	0.0122	0.2297	0.0427
2006–2010	0.0032	0.2353	0.0279	0.0442	0.2559	0.0071	0.3692	0.0571
2000–2004	0.0036	0.2397	0.0379	0.0403	0.6347	0.0133	0.0201	0.0105
2000–2006	0.0022	0.2318	0.0712	0.0228	0.6376	0.0133	0.0161	0.0050
2000–2008	0.0023	0.2814	0.0328	0.0199	0.5069	0.0108	0.1268	0.0192
2000–2010	0.0018	0.2602	0.0310	0.0197	0.3227	0.0914	0.2524	0.0208
2002–2008	0.0022	0.2204	0.0278	0.0222	0.4730	0.1238	0.1103	0.0203
2004–2008	0.0027	0.2089	0.0320	0.0220	0.4829	0.0900	0.1239	0.0377

Table 8. Carl Pearson's K^2 values and χ^2 goodness of fit test values.

	K^2	x^2
2002–2006	1.07×10^5	1.22
2002–2010	1.75×10^5	4.85
2004–2010	1.98×10^5	4.41
2006–2010	1.95×10^5	4.60
2000–2004	0.74×10^5	0.99
2000–2006	1.09×10^5	1.31
2000–2008	1.13×10^5	1.48
2000–2010	1.39×10^5	1.88
2002–2008	1.37×10^5	2.54
2004–2008	0.94×10^5	0.97

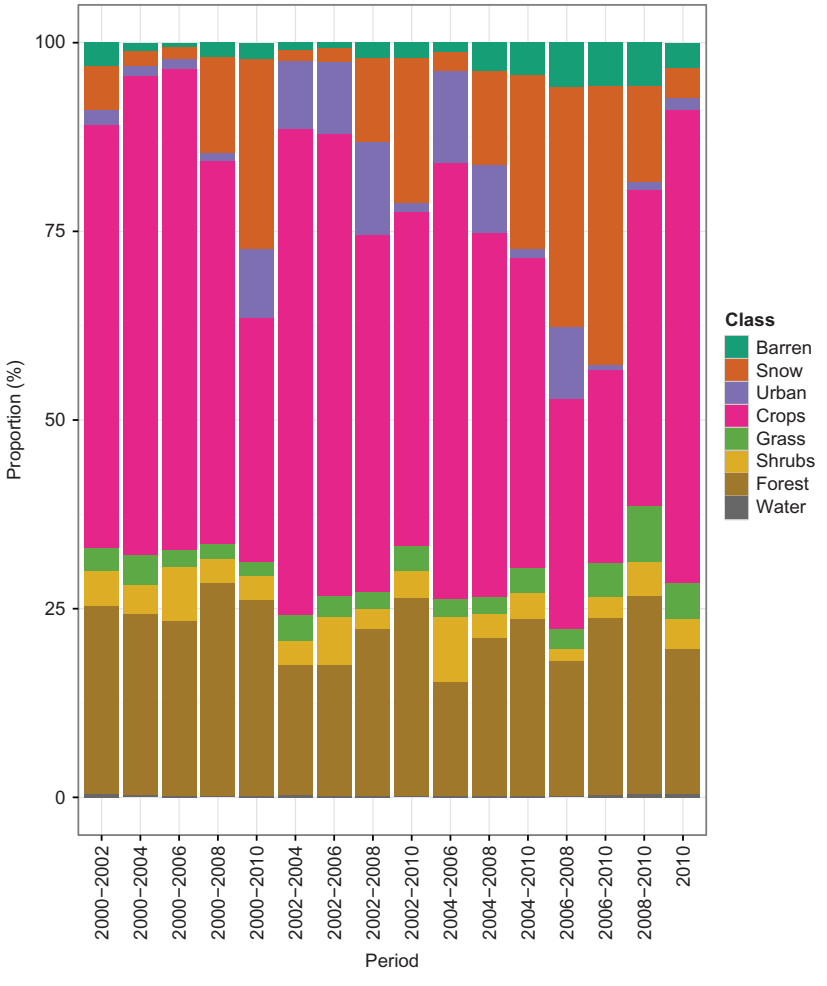

Figure 8. Equilibrium distributions of land cover as they were projected by all transition probability matrices. The calculated proportions of land cover for 2010 are shown to the right for comparison purposes.

Nevertheless, stationarity can be assumed to make scenario-based projections and identify the response of the landscape to management and policy decisions. In the UG basin, the classification results already indicated changes in land-cover trends between the periods examined from 1984 to 2010.

An interesting trend was observed here regarding the 2000–2002 transition matrix: although from 2000 to 2002 we identified a small increase of 0.73% in the agricultural proportion (Figure 4 and Table 2), the equilibrium distributions show a decrease in this proportion, which, from 63.58% in 2002 was reduced to 55.96% (Table 7). The bar plots of Figure 7 illustrate that the only contributors to crops reduction during the period 2000–2002 were conversion to forests (–0.6%) and urban (–1.1%). Therefore, in this case, the agricultural decrease suggested by the equilibrium distributions can be explained by the forest and urban growth noted over the same period (Table 7, 2000–2002 period). The fact that the equilibrium distribution of the 2000–2002 matrix shows an opposite trend in crop

land cover to that observed during the same period highlights that Markovian analysis is not a simple linear extrapolation, but the transition potentials might change over time until equilibrium is reached.

Before developing future projections of land-cover status, we tested our method to examine its accuracy. As a validation measure of the ability to generate future land-cover scenarios under Markov chain analysis, we used transition matrices of years previous to 2010 and generated future scenarios for the year 2010. These scenarios were compared to the historic land-cover map of 2010, as shown in Figure 9 (red indicates land-cover proportion in the historic map). The results indicate that the scenarios generated for 2010 are quite close to the actual historic proportions. Highest overall uncertainties are observed for the land-cover classes forest and shrubs. For instance, the actual proportion of forest in 2010 was 17.12%, while the two most extreme values that we obtained through Markov chain analysis were 19.98 and 15.20% (Figure 9). This gives us confidence for developing other near-future scenarios by applying the same method.

All possible transition probabilities of periods between the years 2000 and 2010, 15 in total, were used to generate 15 different scenarios of future projections for the year 2020 (Figure 10). As the trends in different matrices vary, the future predictions generated were not exactly the same. The date being projected forward is an even multiple of the training periods (see Section 3.3). Therefore, whenever 2020 was not an even multiple of the training period, a simple interpolation (or extrapolation) was used to calculate the proportions for that year.

Figure 11 shows the uncertainty of the projected scenarios. The land-cover types with the highest values of uncertainty were forest and crops, which was expected given that these are the two dominant land-cover types of the study area and the key difference

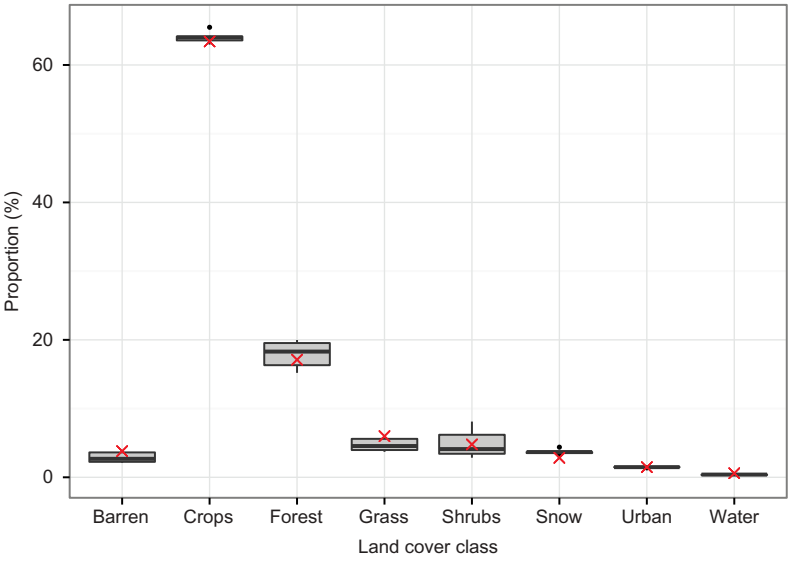

Figure 9. Box plots indicating land-cover trends with uncertainties for 2010, as developed by applying Markov chain analysis. The transition probabilities of years previous to 2010 were used to generate a 2010 scenario. Red denotes actual land-cover proportions for 2010, as derived from the Landsat classifications. The middle bar of each box shows the 50% percentile, while the top and bottom of the box bars show the 75% and 25% percentiles (or first and third quartiles), respectively.

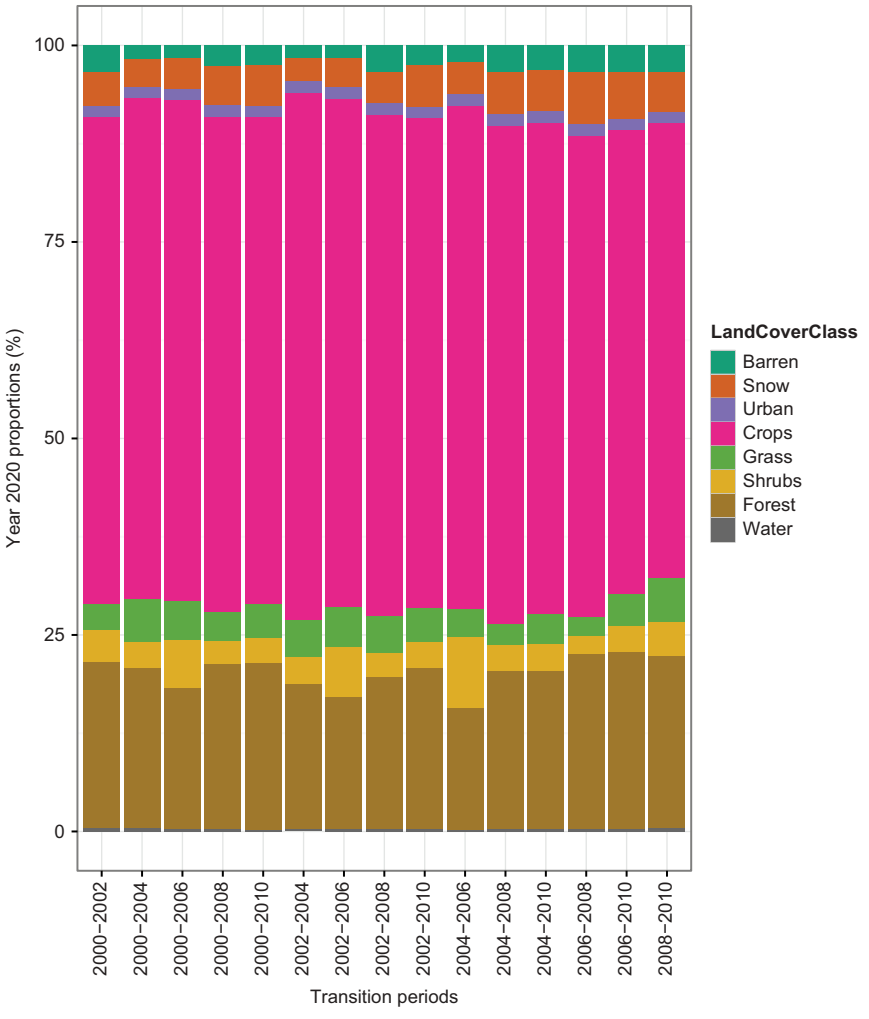

Figure 10. Projected proportions of land cover for 2020, based on the 15 scenarios tested as shown in the *x* axis labels.

between the transition matrices used for future scenarios is that some of them project an expansion of forest and/or agricultural areas while others project a loss in these areas.

Figure 12 shows the spatial distribution of the predicted future land cover for the year 2020 after determining the dominant land-cover types by applying the majority rule in the 15 different scenarios. The main projected trends include forest growth, replacing some of the shrub and grass areas in the mid-northern parts of the UG basin, and less grass and barren lands in the north where snow coverage is greatest. In addition, agricultural expansion and urbanization are projected mainly for the southern parts of the study area.

5. Conclusions

This study detected and quantified trends in land-cover changes by classifying satellite imagery and modelling land-cover change in a region that has undergone one of the

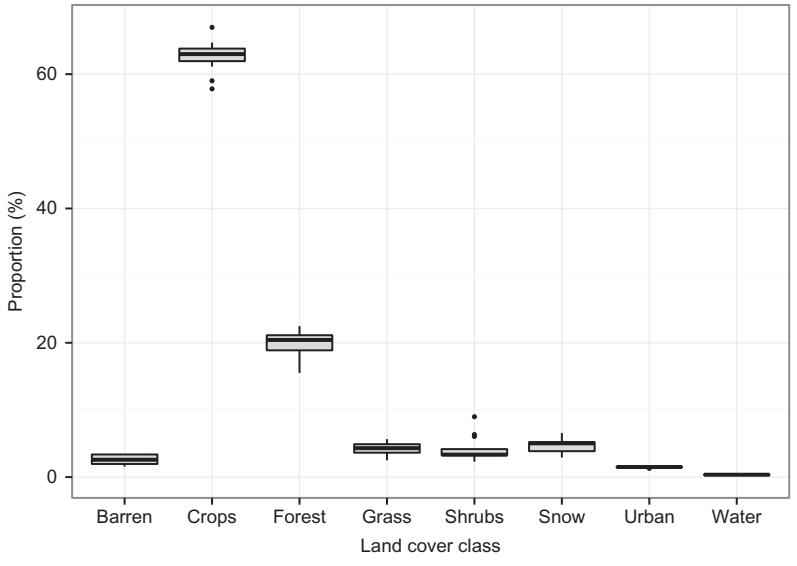

Figure 11. Box plots indicating future land-cover trends with uncertainties in future scenarios for 2020. The results show greater variability in the land-cover types forest and crops, which are the dominant ones in our study area. The middle bar of each box shows the 50% percentile, while the top and bottom of the box bars show the 75% and 25% percentiles (or first and third quartiles), respectively.

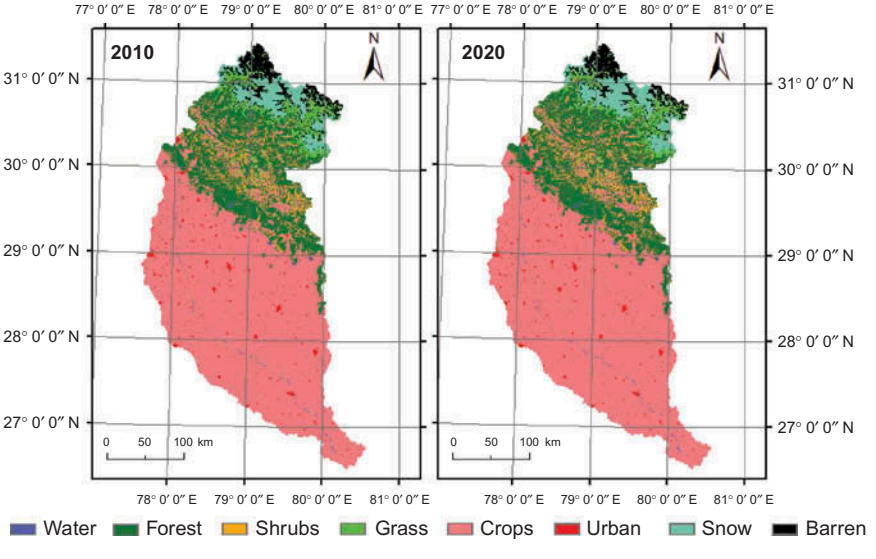

Figure 12. Land-cover maps of historic year 2010 (left) and future scenario for year 2020 (right), as calculated after determining the dominant land-cover types by applying the majority rule in the 15 different scenarios developed by Markov chain analysis.

largest environmental changes in human history over recent decades. India's green revolution, besides its ubiquitous benefits, has resulted in large-scale changes in land cover. Remarkably strong agricultural expansion, development activities, urbanization,

and deforestation have caused alterations and modifications in land-cover status. This is the first study attempting to evaluate and understand the dynamics of land-cover-change processes in this region by monitoring and analysing the spatial patterns of change at a high resolution, which allowed detailed descriptions of land-cover transitions over time.

We focused on a period characterized by dramatic land-cover changes of high complexity. The hypothesis of a stationary system is therefore unreliable and the three future land-cover distributions generated by different transition matrices revealed different trends that do not necessarily represent realistic future states for the UG basin. However, the Markov chain analysis is a simple method for projection of trends and which, regardless of its limitations, can serve as an indicator of the direction and scale of future changes (Bell 1974).

The main trends of changes observed in the study region for the period from 1984 to 2010 are increased areas of forest, agricultural land, and urbanization, and loss of barren, shrubs, and grassland.

Potential future directions of land-cover change in the UG basin vary and depend on the historic time period selected by the analyst to project previous changes into the future. In this study, 15 different scenarios based on historic land-cover change produced different future projections. The scenario using land-cover maps for 2008 and 2010 projects future expansion of forest, urban, grass, and shrubland, with a decline in agriculture and bare soil. More confidence can be placed in this result as it is based on analysis of the most recent land-cover change.

A key limitation of the current approach is that historic trend analysis only considers two discrete points in time. Moreover, Markov chain analysis is unable to assimilate ancillary data, which may constrain the rate and direction of change.

Land-cover change is driven by socio-economic and biophysical factors (Lambin et al. 2001). Therefore, to make valid predictions about future land-cover change it is necessary to understand the causes of historic land-cover change. In the UG, given the observed dependence of the agricultural sector on irrigation, we may hypothesize that an area of land located near an irrigation canal or well is more likely to be converted to cropland than land without a reliable water source. Furthermore, the expansion of cropland may be limited by the presence of the Himalayan mountain range in the north of the basin, where factors such as elevation, aspect, and slope may impose physical limits on crop growth. Understanding the objectives of national and international policies on afforestation in the region may provide a means to constrain future scenarios of change. These examples demonstrate that land-cover change cannot be modelled unless the underlying driving factors are taken into account. Future work will attempt to improve the prediction of land cover by applying modelling approaches that utilize biophysical and socioeconomic datasets. This is a possible way to reduce uncertainty and provide more accurate projections for the future status of land cover in the UG basin.

Acknowledgement

We are grateful to two anonymous reviewers for their constructive comments.

Funding

GMT is financially supported by the Academy of Athens, Greece (Bequest of P. Argyropoulos), and the Grantham Institute for Climate Change. AM and WB are supported by the NERC Changing

Water Cycle (South Asia) project 'Hydro-meteorological feedbacks and changes in water storage and fluxes in Northern India' [grant number NE/I022558/1]. SM is supported by the Grantham Institute for Climate Change.

Supplemental data

The supporting research materials and developed land-cover maps for this article can be accessed after communication with the corresponding author.

References

Anderson, J. R., E. H. Ernest, J. T. Roach, and R. E. Witmer. 1976. "A Land Use and Land Cover Classification System for Use with Remote Sensor Data." US Geological Survey Professional Paper 964. Washington, DC: United States Government Printing Office.

Bell. 1974. "Markov Analysis of Land Use Change-An Application of Stochastic Processes to Remotely Sensed Data." *Socio-Economic Planning Sciences* 8 (6): 311–316. doi:10.1016/0038-0121(74)90034-2.

Bhagyanagar, R., B. M. Kawal, G. S. Dwarakish, and S. Surathkal. 2012. "Land Use/Land Cover Change and Urban Expansion During 1983–2008 in the Coastal Area of Dakshina Kannada District, South India." *Journal of Applied Remote Sensing* 6 (1): 063576. http://dx.doi.org/10.1117/1.JRS.6.063576. doi:10.1117/1.JRS.6.063576.

Bharati, L., and P. Jayakody. 2010." Hydrology of the Upper Ganga River." *International Water-Management Institute*. Project Report No: H043412. http://publications.iwmi.org/pdf/H043412.pdf

Bhatta, B. 2009. "Analysis of Urban Growth Pattern Using Remote Sensing and GIS: A Case Study of Kolkata, India." *International Journal of Remote Sensing* 30 (18): 4733–4746. http://www.tandfonline.com/doi/pdf/10.1080/01431160802651967. http://www.tandfonline.com/doi/abs/10.1080/01431160802651967. doi:10.1080/01431160802651967.

Bourne, L. S. 1976. "Monitoring Change and Evaluating the Impact of Planning Policy on Urban Structure: A Markov Chain Experiment." *Plan Canada* 16: 5–14.

Chavez, P. S. 1989. "Radiometric Calibration of Landsat Thematic Mapper Multispectral Images." *Photogrammetric Engineering and Remote Sensing* 55 (9): 1285–1294.

Chavez, P. S. 1996. "Image-Based Atmospheric Corrections Revisited and Improved." *Pho-Togrammetric Engineering and Remote Sensing* 62 (9): 1025–1036.

Christensen, E. J., J. R. Jensen, E. W. Ramsey, and H. E. Mackey. 1988. "Aircraft MSS Data Registration and Vegetation Classification for Wetland Change Detection." *International Journal of Remote Sensing* 9 (1): 23–38. doi:10.1080/01431168808954834.

Claessens, L., J. M. Schoorl, P. H. Verburg, L. Geraedts, and A. Veldkamp. 2009. "Modelling Interactions and Feedback Mechanisms between Land Use Change and Landscape Processes." *Agriculture, Ecosystems & Environment* 129 (1–3): 157–170. http://www.sciencedirect.com/science/article/pii/S0167880908002417. doi:10.1016/j.agee.2008.08.008.

Cohen, W. B., and S. N. Goward. 2004. "Landsat's Role in Ecological Applications of Remote Sensing." *BioScience* 54 (6): 535–545. doi:10.1641/0006-3568(2004)054[0535:LRIEAO]2.0.CO;2.

Congalton, R. G. 1991. "A Review of Assessing the Accuracy of Classifications of Remotely Sensed Data." *Remote Sensing of Environment* 37 (1): 35–46. doi:10.1016/0034-4257(91)90048-B.

Congalton, R. G. 2010. "How To Assess the Accuracy of Maps Generated from Remotely Sensed Data." In *Manual of Geospatial Science and Technology*. 2nd ed., 403–421. Boca Raton, FL: CRC Press.

Congalton, R., and L. Plourde. 2002. "Quality Assurance and Accuracy Assessment of Information Derived from Remotely Sensed Data." In *Manual of Geospatial Science and Technology*, edited by John Bossler, 349–361. London: Taylor & Francis.

Drewett, J. R. 1969. "A Stochastic Model of the Land Conversion Process." *Regional Studies* 3: 269–280. doi:10.1080/09595236900185281.

Ehlers, M., M. A. Jadkowski, R. R. Howard, and D. E. Brostuen. 1990. "Application of SPOT Data for Regional Growth Analysis and Local-Planning." *Photogrammetric Engineering and Remote Sensing* 56 (2): 175–180.

Ekstrand, S. 1994. "Assessment of Forest Damage with Landsat TM: Correction for Varying Forest Stand Characteristics." *Remote Sensing of Environment* 47 (3): 291–302. doi:10.1016/0034-4257(94)90097-3.

Evenson, R. E., and D. Gollin. 2003. "Assessing the Impact of the Green Revolution, 1960 to 2000." *Science (New York, NY)* 300 (5620): 758–762. doi:10.1126/science.1078710.

FAO. 2010. *Global Forest Resources Assessment 2010: Main Report*. FAO Forestry Paper Series. Report No. 163. Rome: Food and Agriculture Organization of the United Nations.

Forest Survey of India. 2009. "State of Forest Report." *Ministry of Environment and Forests, Govt. of India*, Report No. 11. Dehradun: Forest Survey of India.

Goward, S., T. Arvidson, and D. Williams, J. Faundeen, J. Irons, and S. Franks. 2006. "Historical Record of Landsat Global Coverage: Mission Operations, NSLRSDA, and International Cooperator Stations." *Photogrammetric Engineering & Remote Sensing* 72 (10): 1155–1169. doi:10.14358/PERS.72.10.1155.

Gulati, S. C., and S. Sharma. 2000. *Population Pressure and Deforestation in India*. Delhi: Population Research Centre, Institute of Economic Growth, University Enclave.

Harris, P. M., and S. J. Ventura. 1995. "The Integration of Geographic Data with Remotely-Sensed Imagery to Improve Classification in an Urban Area." *Photogrammetric Engineering and Remote Sensing* 61 (8): 993–998.

Huguenin, R. L., M. A. Karaska, D. VanBlaricom, and J. R. Jensen. 1997. "Subpixel Classification of Bald Cypress and Tupelo Gum Trees in Thematic Mapper Imagery." *Photogrammetric Engineering and Remote Sensing* 63 (6): 717–725.

Indian National Science Academy, Chinese Academy of Sciences, and U.S. National Academy of Sciences. 2001. *Growing Populations, Changing Landscapes: Studies from India, China, and the United States*. Washington, DC: National Academy Press.

Jakubauskas, M. E. 1996. "Thematic Mapper Characterization of Lodgepole Pine Seral Stages in Yellowstone National Park, USA." *Remote Sensing of Environment* 56 (2): 118–132. doi:10.1016/0034-4257(95)00228-6.

Jat, M. K., P. K. Garg, and D. Khare. 2008. "Modelling of Urban Growth Using Spatial Analysis Techniques: A Case Study of Ajmer City (India)." *International Journal of Remote Sensing* 29 (2): 543–567. http://www.tandfonline.com/doi/pdf/10.1080/01431160701280983. http://www.tandfonline.com/doi/abs/10.1080/01431160701280983. doi:10.1080/01431160701280983.

Koster, R. D., P. A. Dirmeyer, Z. Guo, and G. Bonan. 2004. "Regions of Strong Coupling between Soil Moisture and Precipitation." *Science* 305: 1138–1140. doi:10.1126/science.1100217.

Lambin, E. F., and A. H. Strahler. 1994. "Change-Vector Analysis in Multitemporal Space: A Tool to Detect and Categorize Land-Cover Change Processes Using High Temporal-Resolution Satellite Data." *Remote Sensing of Environment* 48 (2): 231–244. doi:10.1016/0034-4257(94)90144-9.

Lambin, E. F., B. L. Turner, H. J. Geist, S. B. Agbola, A. Angelsen, J. W. Bruce, O. T. Coomes, R. Dirzo, G. Fischer, C. Folke, P. S. George, K. Homewood, J. Imbernon, R. Leemans, X. Li, E. F. Moran, M. Mortimore, P. S. Ramakrishnan, J. F. Richards, H. Skånes, W. Steffen, G. D. Stone, U. Svedin, T. A. Veldkamp, C. Vogel, and J. Xu . 2001. "The Causes of Land-Use and Land-Cover Change: Moving Beyond the Myths." *Global Environmental Change* 11: 261–269. doi:10.1016/S0959-3780(01)00007-3.

Lenney, M. P., C. E. Woodcock, J. B. Collins, and H. Hamdi. 1996. "The Status of Agricultural Lands in Egypt: The Use of Multitemporal NDVI Features Derived from Landsat TM." *Remote sensing of environment* 56 (1): 8–20. doi:10.1016/0034-4257(95)00152-2.

Lever, W. F. 1973. "A Markov Approach to the Optimal Size of Cities in England and Wales." *Urban Studies* 10: 353–365. doi:10.1080/00420987320080481.

Liu, D., K. Song, J. R. G. Townshend, and P. Gong. 2008. "Using Local Transition Probability Models in Markov Random Fields for Forest Change Detection." *Remote Sensing of Environment* 112 (5): 2222–2231. Earth Observations for Terrestrial Biodiversity and Ecosystems Special Issue. http://www.sciencedirect.com/science/article/pii/S0034425707004476. doi:10.1016/j.rse.2007.10.002.

Lu, D., P. Mausel, E. Brondízio, and E. Moran. 2004. "Change Detection Techniques." *International Journal of Remote Sensing* 25 (12): 2365–2401. doi:10.1080/0143116031000139863.

Meehl, G. A. 1994. "Influence of the Land Surface in the Asian Summer Monsoon: External Conditions Versus Internal Feedbacks." *Journal of Climate* 7: 1033–1049. doi:10.1175/1520-0442(1994)007<1033:IOTLSI>2.0.CO;2.

Michener, W. K., and P. F. Houhoulis. 1997. "Detection of Vegetation Changes Associated with Extensive Flooding in a Forested Ecosystem." *Photogrammetric Engineering and Remote Sensing* 63 (12): 1363–1374.

Moghadam, H. S., and M. Helbich. 2013. "Spatiotemporal Urbanization Processes in the Megacity of Mumbai, India: A Markov Chains-Cellular Automata Urban Growth Model." *Applied Geography* 40 (0): 140–149. http://www.sciencedirect.com/science/article/pii/S0143622813000362. doi:10.1016/j.apgeog.2013.01.009.

Moran, M. S., R. D. Jackson, P. N. Slater, and P. M. Teillet. 1992. "Evaluation of Simplified Procedures for Retrieval of Land Surface Reflectance Factors from Satellite Sensor Output." *Remote Sensing of Environment* 41 (2–3): 169–184. doi:10.1016/0034-4257(92)90076-V.

Muller, M. R., and J. Middleton. 1994. "A Markov Model of Land-Use Change Dynamics in the Niagara Region, Ontario, Canada." *Landscape Ecology* 9 (2): 151–157.

Office of the Registrar General & Census Commissioner, India. 2011. "Census-2011." Accessed June 2013. http://www.censusindia.gov.in

O'Keeffe, J., N. Kaushal, V. Smakhtin, and L. Bharati. 2012. "Assessment of Environmental Flows for the Upper Ganga Basin." Summary Report, WWF-India, New Delhi. http://awsassets.wwfindia.org/downloads/wwf_e_flows_report.pdf

Parker, D. C., S. M. Manson, M. A. Janssen, M. J. Hoffmann, and P. Deadman. 2003. "Multi-Agent Systems for the Simulation of Land-Use and Land-Cover Change: A Review." *Annals of the Association of American Geographer*s 93 (2): 314–337. doi:10.1111/1467-8306.9302004.

Petit, C., T. Scudder, and E. Lambin. 2001. "Quantifying Processes of Land-Cover Change by Remote Sensing: Resettlement and Rapid Land-Cover Changes in South-Eastern Zambia." *International Journal of Remote Sensing* 22 (17): 3435–3456. doi:10.1080/01431160010006881.

Pinstrup-Andersen, P., and P. B. R. Hazell. 1985. "The Impact of the Green Revolution and Prospects for the Future." *Food Reviews International* 1 (1): 1–25. doi:10.1080/87559128509540765.

Pitman, A. J. 2003. "The Evolution of, and Revolution in, Land Surface Schemes Designed for Climate Models." *International Journal of Climatology* 23 (5): 479–510. doi:10.1002/joc.893.

Rahman, A., S. Kumar, S. Fazal, and M. A. Siddiqui. 2012. "Assessment of Land Use/Land Cover Change in the North-West District of Delhi using Remote Sensing and GIS Techniques." *Journal of the Indian Society of Remote Sensing* 40 (4): 689–697. http://dx.doi.org/10.1007/s12524-011-0165-4. doi:10.1007/s12524-011-0165-4.

Rai, S., E. Sharma, and R. Sundriyal. 1994. "Conservation in the Sikkim Himalaya: Traditional Knowledge and Land-Use of the Mamlay Watershed." *Environmental Conservation* 21 (01): 30–56. doi:10.1017/S0376892900024048.

Raja, R. A., V. Anand, A. Senthil Kumar, S. Maithani, and V. Abhai Kumar. 2013. "Wavelet Based Post Classification Change Detection Technique for Urban Growth Monitoring." *Journal of the Indian Society of Remote Sensing* 41 (1): 35–43. http://dx.doi.org/10.1007/s12524-011-0199-7. doi:10.1007/s12524-011-0199-7.

Rajitha, K., C. K. Mukherjee, R. Vinu Chandran, and M. M. Prakash Mohan. 2010. "Land-Cover Change Dynamics and Coastal Aquaculture Development: A Case Study in the East Godavari Delta, Andhra Pradesh, India Using Multi-Temporal Satellite Data." *International Journal of Remote Sensing* 31 (16): 4423–4442. http://www.tandfonline.com/doi/pdf/10.1080/01431160903277456. http://www.tandfonline.com/doi/abs/10.1080/01431160903277456. doi:10.1080/01431160903277456.

Rao, K. S., and R. Pant. 2001. "Land Use Dynamics and Landscape Change Pattern in a Typical Micro Watershed in the Mid Elevation Zone of Central Himalaya, India." *Agriculture Ecosystems & Environment* 86 (2): 113–124. doi:10.1016/S0167-8809(00)00274-7.

Ravindranath, N. H., R. K. Chaturvedi, and I. K. Murthy. 2008. "Forest Conservation, Afforestation and Reforestation in India: Implications for Forest Carbon Stocks." *Current Science* 95 (2): 216–222.

Renwick, A., T. Jansson, P. H. Verburg, C. Revoredo-Giha, W. Britz, A. Gocht, and D. Mc-Cracken. 2013. "Policy Reform and Agricultural Land Abandonment in the EU." *Land Use Policy* 30 (1): 446–457. doi:10.1016/j.landusepol.2012.04.005.

Rouse, J. W., R. H. Jr Haas, J. A. Schell, and D. W. Deering. 1974. "Monitoring Vegetation Systems in the Great Plains with ERTS" NASA SP-351, Third ERTS-1 symposium NASA, Washington, DC, 309317.

Sader, S. A. 1987. "Digital Image Classification Approach for Estimating Forest Clearing and Regrowth Rates and Trends." *International Geoscience and Remote Sensing Symposium* 1: 209213.

Schoorl, J. M., A. Veldkamp, and J. Bouma. 2002. "Modeling Water and Soil Redistribution in a Dynamic Landscape Context." *Soil Science Society of America Journal* 66: 1610–1619. https://www.soils.org/publications/sssaj/abstracts/66/5/1610. doi:10.2136/sssaj2002.1610.

Semwal, R. L., S. Nautiyal, K. K. Sen, U. Rana, R. K. Maikhuri, K. S. Rao, and K. G. Saxena. 2004. "Patterns and Ecological Implications of Agricultural Land-Use Changes: A Case Study from Central Himalaya, India." *Agriculture Ecosystems & Environment* 102 (1): 81–92. doi:10.1016/S0167-8809(03)00228-7.

Seneviratne, S. I., T. Corti, E. L. Davin, M. Hirschi, E. B. Jaeger, I. Lehner, B. Orlowsky, and A. J. Teuling. 2010. "Investigating Soil Moisture-Climate Interactions in a Changing Climate: A Review." *Earth-Science Reviews* 99 (3–4): 125–161. doi:10.1016/j.earscirev.2010.02.004.

Sen Roy, S., R. Mahmood, D. Niyogi, M. Lei, S. A. Foster, K. G. Hubbard, E. Douglas, and R. Pielke Sr. 2007. "Impacts of the Agricultural Green Revolution – Induced Land Use Changes on Air Temperatures in India." *Journal of Geophysical Research* 112: D21.

Sen Roy, S., R. Mahmood, A. I. Quintanar, and A. Gonzalez. 2011. "Impacts of Irrigation on Dry Season Precipitation in India." *Theoretical and Applied Climatology* 104 (1–2): 193–207. doi:10.1007/s00704-010-0338-z.

Sheeja, R. V., S. Joseph, D. S. Jaya, and R. S. Baiju. 2011. "Land Use and Land Cover Changes Over a Century (1914–2007) in the Neyyar River Basin, Kerala: A Remote Sensing and GIS Approach." *International Journal of Digital Earth* 4 (3): 258–270. http://www.tandfonline.com/doi/pdf/10.1080/17538947.2010.493959. doi:10.1080/17538947.2010.493959.

Singh, A. 1989. "Review Article Digital Change Detection Techniques using Remotely-Sensed Data." *International Journal of Remote Sensing* 10 (6): 989–1003. doi:10.1080/01431168908903939.

Singh, R. B. 2000. "Environmental Consequences of Agricultural Development: A Case Study from the Green Revolution State of Haryana, India." *Agriculture, Ecosystems & Environment* 82: 97–103. doi:10.1016/S0167-8809(00)00219-X.

Sohl, T. L., and P. R. Claggett. 2013. "Clarity Versus Complexity: Land-Use Modeling as a Practical Tool Fordecision-Makers." *Journal of Environmental Management* 129 (0): 235–243. http://www.sciencedirect.com/science/article/pii/S0301479713005069. doi:10.1016/j.jenvman.2013.07.027.

Song, C., C. E. Woodcock, K. C. Seto, M. P. Lenney, and S. A. Ma-comber. 2001. "Classification and Change Detection Using Landsat TM Data: When and How to Correct Atmospheric Effects?" *Remote Sensing of Environment* 75 (2): 230–244. doi:10.1016/S0034-4257(00)00169-3.

Spanner, M. A., L. L. Pierce, D. L. Peterson, and S. W. Running. 1990. "Remote Sensing of Temperate Coniferous Forest Leaf Area Index The Influence of Canopy Closure, Understory Vegetation and Background Reflectance." *International Journal of Remote Sensing* 11 (1): 95–111. doi:10.1080/01431169008955002.

Takada, T., A. Miyamoto, and S. F. Hasegawa. 2010. "Derivation of a Yearly Transition Probability Matrix for Land-Use Dynamics and Its Applications." *Landscape Ecology* 25: 561–572. doi:10.1007/s10980-009-9433-x.

Tayyebi, A. H., A. Tayyebi, and N. Khanna. 2014. "Assessing Uncertainty Dimensions in Land-Use Change Models: Using Swap and Multiplicative Error Models for Injecting Attribute and Positional Errors in Spatial Data." *International Journal of Remote Sensing* 35 (1): 149–170. http://www.tandfonline.com/doi/abs/10.1080/01431161.2013.866293. doi:10.1080/01431161.2013.866293.

Thenkabail, P. S., M. Schull, and H. Turral. 2005. "Ganges and Indus River Basin Land Use/Land Cover (LULC) and Irrigated Area Mapping Using Continuous Streams of MODIS Data." *Remote Sensing of Environment* 95 (3): 317–341. doi:10.1016/j.rse.2004.12.018.

University of Oklahoma. 2011. "Global Geo-Referenced Field Photo Library." Accessed May 2012. http://www.eomf.ou.edu/photos/.

Verburg, P. H., B. Eickhout, and H. Meijl. 2008. "A multi-Scale, Multi-Model Approach for Analyzing the Future Dynamics of European Land Use." *The Annals of Regional Science*

42 (1): 57–77. http://dx.doi.org/10.1007/s00168-007-0136-4. doi:10.1007/s00168-007-0136-4.

Verburg, P. H., T. Huajun, W. Wenbin, Y. Peng, and C. Youqi. 2009. "Recent Progresses of Land Use and Land Cover Change (LUCC) Models." *Acta Geographica Sinica* 64: 456–468.

Verburg, P. H., W. Soepboer, A. Veldkamp, R. Limpiada, V. Es-paldon, and S. S. A. Mastura. 2002. "Modeling the Spatial Dynamics of Regional Land Use: The CLUE-s Model." *Environmental Management* 30 (3): 391–405. http://dx.doi.org/10.1007/s00267-002-2630-x. doi:10.1007/s00267-002-2630-x.

Verghese, B. G. 1993. *Harnessing the Eastern Himalayan Rivers: Regional Cooperation in South Asia*. Delhi: Konark Publishers.

Weng, Q. 2002. "Land Use Change Analysis in the Zhujiang Delta of China Using Satellite Remote Sensing, GIS and Stochastic Modelling." *Journal of Environmental Management* 64 (3): 273–284.

Westhoek, H. J., M. van den Berg, and J. A. Bakkes. 2006. "Scenario Development to Explore the Future of Europe's Rural Areas." *Agriculture, Ecosystems & Environment* 114 (1): 7–20. http://www.sciencedirect.com/science/article/pii/S0167880905005311. doi:10.1016/j.agee.2005.11.005.

Westmoreland, S., and D. A. Stow. 1992. "Category Identification of Changed Land-Use Polygons in an Integrated Image Processing/Geographic Information System." *Photogrammetric Engineering and Remote Sensing* 58: 15931599.

Wu, Q., H.-Q. Li, R.-S. Wang, J. Paulussen, Y. He, M. Wang, B.-H. Wang, and Z. Wang. 2006. "Monitoring and Predicting Land Use Change in Beijing Using Remote Sensing and GIS." *Landscape and Urban Planning* 78 (4): 322–333. doi:10.1016/j.landurbplan.2005.10.002.

Yeh, A. G. O., and X. Li. 1999. "Economic Development and Agricultural Land Loss in the Pearl River Delta, China." *Habitat International* 23: 373390.